Journal of Solid State Chemistry 183 (2010) 2862–2868

Contents lists available at ScienceDirect

Journal of Solid State Chemistry

journal homepage: www.elsevier.com/locate/jssc

A series of new supramolecular structures constructed from triethylenediamine and different polyoxometalates

Yan Wang [a], Cheng-Ling Pan [b], Li-Na Xiao [a], Feng-Qing Wu [a], Hong Ding [a], Ya-Bing Liu [a], Zhong-Min Gao [a], Da-Fang Zheng [a], Tie-Gang Wang [a], Guang-Di Yang [a], Xiao-Bing Cui [a,*], Ji-Qing Xu [a,*]

[a] College of Chemistry and State Key Laboratory of Inorganic Synthesis and Preparative Chemistry, Jilin University, Changchun, Jilin, PR China
[b] College of Chemistry, Chongqing Normal University, Chongqing 400047, China

ARTICLE INFO

Article history:
Received 17 June 2010
Received in revised form
8 September 2010
Accepted 26 September 2010
Available online 1 October 2010

Keywords:
Polyoxometalates
Hydrothermal synthesis
Triethylenediamine
Supramolecular compounds

ABSTRACT

Three new supramolecular compounds based on triethylenediamine and different polyoxometalates $[W_3^{VI}V_3^{V}O_{19}H]\{[Cu(HDABCO)]_2(H_2O)\}$ (**1**), $[P_2Mo_{18}^{VI}O_{62}][HDABCO]_2[H_2DABCO]_2\cdot 12\,H_2O$ (**2**) and $[Mo_{7.5}^{VI}W_{0.5}^{VI}O_{27}][Cu(HDABCO)]_2\cdot 2\,H_3O\cdot 2\,H_2O$ (**3**) (DABCO=triethylenediamine) have been synthesized hydrothermally and characterized by IR, TG, XPS and X-ray diffraction analyses. Crystal structure analyses reveal that compound **1** exhibits a face-centered cubic packing motif, compound **2** displays a supramolecular structure constructed form the "chains" arranged hexagonally, compound **3** contains $[Mo_{7.5}W_{0.5}O_{27}]_\infty$ chain decorated by $[Cu(HDABCO)]^{2+}$ cations, which was then packed into a layer structure. These results show that the same organonitrogen combining with the different POMs will yield different supramolecular networks.

1. Introduction

In the past 30 years, supramolecular chemistry has developed at a tremendous rate. This expansion has been driven by the growing knowledge regarding synthetic and characterization methods for complex structures [1]. The directed assembly of supramolecular arrays from discrete molecular building blocks is a topic of significant interest with potential applications in the areas of catalysis, molecular electronics, sensor design and optics [2,3]. In the construction of supramolecular materials, one important strategy is that those of low-dimensional building blocks extend to high-dimensional networks through weak intermolecular interactions, including hydrogen bonding, $\pi\cdots\pi$ stacking and weak van der Waals interactions, etc. Doubtless, the hydrogen bond is the most familiar organizing force in supramolecular assemblies by virtue of its unique strength and directionality that may control short-range packing [4].

Polyoxometalates (POMs), as a kind of significant metal oxide clusters with abundant topologies [5], have recently been employed as discrete building blocks for constructing supramolecular arrays with various organic moieties [6]. Supramolecular assemblies based on POMs have been intensively investigated in many important aspects such as catalysis, non-linear optical material and medicine [7]. In most cases, available nucleophilic oxygen atoms on the surface of POMs as hydrogen acceptors interact with oxygen, nitrogen or carbon atoms of organic moieties as hydrogen donors to form O–H···O, N–H···O or C–H···O hydrogen bonds for constructing high-dimensional supramolecular networks. In contrast, less attention was paid to the regulatory effects of POMs and organic ligands in the supramolecular network [8], despite these having been demonstrated to play a key role in controlling the topological structures of supramolecular architectures.

On the other hand, a great deal of organic moieties has been introduced to combine with POMs for constructing supramolecular architectures. There is a synergism between organic and inorganic components, so that the combination of various organic and inorganic components will result in different supramolecular arrangements. Though many organonitrogen compounds including tetra-alkyl-ammonium, ethylenediamine, diethylamine, triethylamine, etc. have been used as organic components of supramolecular architectures [6,7], to the best of our knowledge, it is surprising that supramolecular architectures containing triethylenediamine as organic components combined with POMs are rather scarce [9].

As a continuous work, here we report three new supramolecular networks based on triethylenediamine and different POMs: $[W_3^{VI}V_3^{V}O_{19}H]\{[Cu(HDABCO)]_2(H_2O)\}$ (**1**), $[P_2Mo_{18}^{VI}O_{62}][HDABCO]_2[H_2DABCO]_2\cdot 12\,H_2O$ (**2**) and $[Mo_{7.5}^{VI}W_{0.5}^{VI}O_{27}][Cu(HDABCO)]_2\cdot 2\,H_3O\cdot 2\,H_2O$ (**3**) (DABCO=triethylenediamine). The three compounds represent interesting examples of supramolecular architectures constructed from DABCO and different POMs.

* Corresponding authors.
E-mail addresses: cuixb@mail.jlu.edu.cn (X.-B. Cui), xjq@mail.jlu.edu.cn (J.-Q. Xu).

0022-4596/$ - see front matter © 2010 Elsevier Inc. All rights reserved.
doi:10.1016/j.jssc.2010.09.038

Compound **1** exhibits a face-centered cubic packing motif, Compound **2** displays a supramolecular structure constructed form the "chains" arranged hexagonally, compound **3** contains $[Mo_{7.5}W_{0.5}O_{27}]_\infty$ chain decorated by $[Cu(HDABCO)]^{2+}$ cations, which was then packed into a layer structure. These results show that the same organonitrogen combining with the different POMs will yield different supramolecular networks.

2. Experimental

2.1. General methods

All reagents were purchased commercially and used without further purification. The elemental analyses (C, H and N) were performed on a Perkin-Elmer 2400 CHN elemental analyzer. The elemental analyses (W, V, Mo and Cu) were performed on a Perkin-Elmer Optima 3300DV spectrophotometer. The infrared spectra were recorded with a Perkin-Elmer SPECTRUM ONE FTIR spectrometer with KBr pellets in the 4000–200 cm^{-1} region. XPS measurements were performed on single crystals with ESCALAB MARK II apparatus, using the Mg$K\alpha$ (1253.6 eV) achromatic X-ray radiation source. The powder XRD patterns were obtained with a Scintag X1 powder diffractometer system using Cu$K\alpha$ radiation with a variable divergent slit and a solid-state detector. Thermogravimetric analysis (TG) data were recorded with a thermal analysis instrument (SDT 2960, TA Instruments, New Castle, DE, USA) with the heating rate of 10 °C min^{-1} in an air flow.

2.2. Synthesis

Synthesis of $[W_3^{VI}V_3^{V}O_{19}H]\{[Cu(HDABCO)]_2(H_2O)\}$ (**1**): Compound **1** was synthesized hydrothermally by reacting of $Na_2WO_4\cdot 2H_2O$ (0.5 g, 1.5 mmol), H_3BO_3 (0.1 g, 1.6 mmol), NH_4VO_3 (0.2 g, 1.7 mmol), $CuCl_2\cdot 2H_2O$ (0.3 g, 1.7 mmol), DABCO (0.33 g, 1.5 mmol) and distilled water (15 ml) in an 18 ml Teflon-lined autoclave. The pH of the mixture was necessarily adjusted to 5 with HCl solution. The mixture was heated under autogenous pressure at 160 °C for 5 days and then left to cool to room temperature. Orange crystals could be isolated in about 55% yield (based on W). We also tried to synthesize compound **1** without the addition of H_3BO_3, which is not successful yet. Anal. calcd. for $C_{12}H_{29}Cu_2N_4O_{20}V_3W_3$: C, 10.44; H, 2.12; N, 4.06; W, 39.94; Cu, 9.20; V, 11.07%. Found: C, 9.90; H, 2.08; N, 4.06; W, 40.06; Cu, 9.35; V, 11.91%. IR (cm^{-1}): 3436, 3020, 1611, 1475, 1381, 1320, 1219, 1166, 1054, 982, 945, 840, 783, 587, 445.

Synthesis of $[P_2Mo_{18}^{VI}O_{62}][HDABCO]_2[H_2DABCO]_2\cdot 12H_2O$ (2): Compound **2** was synthesized hydrothermally by reacting of $Na_2WO_4\cdot 2H_2O$ (0.5 g, 1.5 mmol), $(NH_4)_6Mo_7O_{24}\cdot 4H_2O$ (0.33 g, 0.2 mmol), $CuCl_2\cdot 2H_2O$ (0.3 g, 1.7 mmol), KH_2PO_4 (0.2 g, 1.5 mmol), DABCO (0.33 g, 1.5 mmol) and distilled water (15 ml) in an 18 ml Teflon-lined autoclave. The pH of the mixture was necessarily adjusted to 5 with $NH_3\cdot H_2O$ solution. The mixture was heated under autogenous pressure at 160 °C for 5 days and then left to cool to room temperature. Black crystals could be isolated in about 52% yield (based on Mo). We also tried to synthesize compound **2** without the addition of $Na_2WO_4\cdot 2H_2O$ and/or $CuCl_2\cdot 2H_2O$, which is not successful yet. Anal. calcd. for $C_{24}H_{78}Mo_{18}N_8O_{74}P_2$: C, 8.35; H, 2.28; N, 3.25; Mo, 50.03; P, 1.79%. Found: C, 8.01; H, 2.22; N, 3.54; W, 50.06; P, 1.81%. IR (cm^{-1}): 3422, 3196, 3065, 3019, 2619, 2339, 1621, 1467, 1405, 1320, 1166, 1078, 1054, 1003, 935, 896, 810, 764, 611, 567, 516 and 384.

Synthesis of $[Mo_{7.5}^{VI}W_{0.5}^{VI}O_{27}][Cu(HDABCO)]_2\cdot 2H_3O\cdot 2H_2O$ (**3**): Compound **3** was synthesized hydrothermally by reacting of $Na_2WO_4\cdot 2H_2O$ (0.5 g, 1.5 mmol), $(NH_4)_6Mo_7O_{24}\cdot 4H_2O$ (0.33 g, 0.2 mmol), $Cu(NO_3)\cdot 3H_2O$ (0.4 g, 1.6 mmol), $C_2H_2O_4\cdot 2H_2O$ (0.2 g, 1.6 mmol), DABCO (0.33 g, 1.5 mmol) and distilled water (15 ml) in an 18 ml Teflon-lined autoclave. The pH of the mixture was necessarily adjusted to 6 with $NH_3\cdot H_2O$ solution. The mixture was heated under autogenous pressure at 160 °C for 5 days and then left to cool to room temperature. Black crystals could be isolated in about 23% yield (based on Mo). Anal. calcd. for $C_{12}H_{36}Cu_2Mo_{7.5}N_4O_{31}W_{0.5}$: C, 8.63; H, 2.17; N, 3.35; W, 5.50; Mo, 43.06; Cu, 7.61%. Found: C, 8.91; H, 2.41; N, 3.40; W, 5.64; Mo, 42.23; Cu, 7.35%. IR (cm^{-1}): 3437, 3018, 1653, 1464, 1386, 1363, 1318, 1225, 1163, 1050, 999, 918, 880, 825, 708, 654, 579, 495 and 421.

2.3. X-ray crystallographic study

Reflection intensity data for **1**, **2** and **3** were collected on a Bruker Apex II diffractometer equipped with graphite monochromated Mo$K\alpha$ radiation (λ=0.71073 Å) at room temperature, respectively. All structures were solved by direct methods and refined using full-matrix least squares technique on F^2 using SHELXTL-97 crystallographic software package. Anisotropic thermal parameters were refined for all non-hydrogen atoms, except C12 in **1** and C1, C2 and O4w in **2** for severe disorder. All hydrogen atoms of the carbon atoms of the ligands were placed in geometrically calculated positions and refined with fixed isotropic displacement parameters using a riding model, and those of the nitrogen atoms of the ligands and waters were not located. Crystallographic data and structure refinements for **1**–**3** are given in Table 1. CCDC numbers: 779,889 for **1**, 777,890 for **2** and 777,891 for **3**.

3. Results and discussion

3.1. Description of crystal structures

Structure of 1: The X-ray crystallographic study reveals that **1** consists of protonated $[W_3^{VI}V_3^{V}O_{19}H]^{4-}$ clusters and transition metal coordination fragments $\{Cu(HDABCO)]_2(H_2O)\}^{4+}$. The $[W_3^{VI}V_3^{V}O_{19}H]^{4-}$ anion exhibits a centrosymmetric M_6O_{19} structure in which the metal atoms (disorderly occupied by tungsten and vanadium atoms with equivalent occupancy factor of 0.5) are octahedrally arranged about a central oxygen atom. In addition, each metal atom is also bonded to four bridging oxygen atoms and one terminal oxygen ligand, ensuring octahedral coordination about each metal center. They describe a structure of nearly perfect octahedral symmetry. The M_6O_{19} structure has been known for a long time, which include the isopolyanions such as $[Nb_6O_{19}]^{8-}$ [5a], $[Ta_6O_{19}]^{8-}$ [5a], $[Mo_6O_{19}]^{2-}$ [5a], $[W_6O_{19}]^{2-}$ [5a], $[V_6O_{19}]^{8-}$ [10] and mixed isopolyanions such as $[V_2W_4O_{19}]^{4-}$ [5a], $[Nb_3W_3O_{19}]^{5-}$ [5a], etc. Compound **1** is based on the $[W_3^{VI}V_3^{V}O_{19}H]^{4-}$ anion, which contains one protons that could not be located by the X-ray crystallographic analysis. Such anions are common especially in the field of polyoxometalates [5,11].

The M–O distances of the $[W_3^{VI}V_3^{V}O_{19}H]^{4-}$ anion can be grouped into three sets: $M-O_t$ with bond distance of 1.66(2) Å, $M-O_b$ with bond distances of 1.85(2)–1.95(2) Å and $M-O_c$ with bond distance of 2.3044(15) Å. Bond valence sums (BVS) for the tungsten, the vanadium and the copper atoms of **1** were calculated [12,13]. Results for the independent tungsten atom W1, the independent vanadium atom V1 and the independent copper atom Cu1 are 6.20, 4.73 and 0.73, respectively, which reveals that the oxidation states for the tungsten atoms, the

Table 1
Crystal data and structural refinements for compounds **1**, **2** and **3**.

Empirical formula	$C_{12}H_{29}Cu_2N_4O_{20}V_3W_3$	$C_{24}H_{78}Mo_{18}N_8O_{74}P_2$	$C_{12}H_{36}Cu_2Mo_{7.5}N_4O_{31}W_{0.5}$
Formula weight	1380.83	3451.80	1671.02
Crystal system	Cubic	Hexagonal	Triclinic
Space group	$Pa\bar{3}$	$P\bar{6}2c$	$P\bar{1}$
a (Å)	14.0558(2)	13.2621(3)	9.5347(19)
b (Å)	14.0558(2)	13.2621(3)	10.301(2)
c (Å)	14.0558(2)	29.5837(11)	11.614(2)
α (deg)	90	90	105.22(3)
β (deg)	90	90	102.60(3)
γ (deg)	90	120	100.35(3)
Volume (Å^3)	2776.94(7)	4506.2(2)	1039.6(3)
Z	4	2	1
D_c (Mg m^{-3})	3.303	2.544	2.669
μ (mm^{-1})	14.929	2.561	4.656
F(000)	2551	3316	794
θ for data collection	2.51–26.02	1.90–26.05	3.25–27.48
Limiting indices	$-17<=h<=14$ $-17<=k<=15$ $-17<=l<=14$	$-15<=h<=16$, $-13<=k<=16$, $-24<=l<=36$	$-12<=h<=12$, $-11<=k<=13$, $-15<=l<=13$
Reflections collected	14,431	24,315	10,299
Reflections unique	922 [R(int)=0.0559]	3051[R(int)=0.0418]	4720 [R(int)=0.0600]
Completeness to θ	100.0%	99.9%	98.8%
Data/parameters	922/69	3051/ 169	4720/254
GOF on F^2	1.336	1.176	1.043
R^a [$I>2\sigma(I)$]	R_1=0.0998 ωR_2=0.2279	R_1=0.0564 ωR_2=0.1419	R_1=0.0615 ωR_2=0.1615
R^b (all data)	R_1=0.1038 ωR_2=0.2294	R_1=0.0574 ωR_2=0.1425	R_1=0.0666 ωR_2=0.1650

[a] $R1=\Sigma\big||F_o|-|F_c|\big|/\Sigma|F_o|$.
[b] $\omega R_2=\{\Sigma[w\,(F_o^2-F_c^2)^2]/\Sigma[w(F_o^2)^2]\}^{1/2}$.

vanadium atoms and the copper atoms are +6, +5 and +1, respectively. Thus the formula for **1** is $[W_3^{VI}V_3^{V}O_{19}H]^{4-}$.

The Cu1 center was coordinated by an oxygen atom from the water molecule (Cu–Ow bond: 1.91(8) Å) and a nitrogen atom from the DABCO ligand (Cu–N bonds: 2.05(4) Å) linearly. The oxygen from the water molecule acts as a bridge joining two Cu1 centers, forming a $\{Cu(HDABCO)]_2(H_2O)\}^{4+}$ cation. It should be noted that the oxygen of the water molecule is disorderedly distributed at two positions with equivalent occupancy factor of 0.5, respectively, so that there is an inversion center located at the midpoint of the two halves of disordered oxygen atoms. Alternatively, the disordered oxygen atom links the two [Cu(HDABCO)]$^{4+}$ cations linearly into a dumbbell-shape structure.

As shown in Fig. 1, compound **1** exhibits a face-centered cubic packing (FCC) motif. The big ball represents the $[W_3^{VI}V_3^{V}O_{19}H]^{4-}$ anion, if we omit all the $\{Cu(HDABCO)]_2(H_2O)\}^{4+}$ cations, it is very clear that $[W_3^{VI}V_3^{V}O_{19}H]^{4-}$ anions pack in a FCC packing motif. Detailed analysis of the packing motif reveals that there are a $\{Cu(HDABCO)]_2(H_2O)\}^{4+}$ cation and six halves of $\{Cu(HDABCO)]_2(H_2O)\}^{4+}$ cations in the cubic unit. It should be noted that the diagonal line of the cubic unit just passes through two Cu1 centers, the disordered oxygen atoms and the nitrogen atoms of the DABCO ligands of the $\{Cu(HDABCO)]_2(H_2O)\}^{4+}$ cation, so that the midpoint of the two halves of the disordered oxygen atoms is just the inversion center of the cubic unit.

As shown in Fig. 1, there are eight DABCO ligands in the cubic unit, each of which in the dumbbell-shape $\{Cu(HDABCO)]_2(H_2O)\}^{4+}$ cation is located at the center of the tetrahedron constructed from four $[W_3^{VI}V_3^{V}O_{19}H]^{4-}$ anions, as shown in Fig. 2.

Crystallographic analysis reveals that the packing of **1** comes from the complex hydrogen bonding interactions between the carbon atoms of the DABCO ligands and the oxygen atoms of the $[W_3^{VI}V_3^{V}O_{19}H]^{4-}$ anions. There are only two crystallographically independent carbon atoms C(1) and C(2), the C(1) (and its symmetry equivalents) as hydrogen donors interacts with the O(3)($-y$,0.5+z,$-$0.5$-x$) (and its symmetry equivalents) as the hydrogen acceptor with bond distance of 3.24(4) Å, while

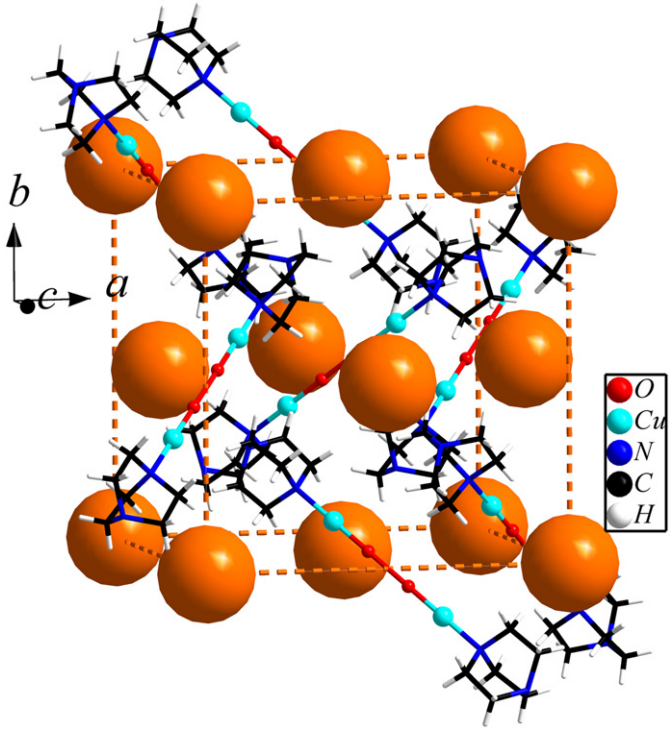

Fig. 1. The topological representation of the FCC packing motif in compound **1**. The big ball represents the $[W_3^{VI}V_3^{V}O_{19}H]^{4-}$ anions.

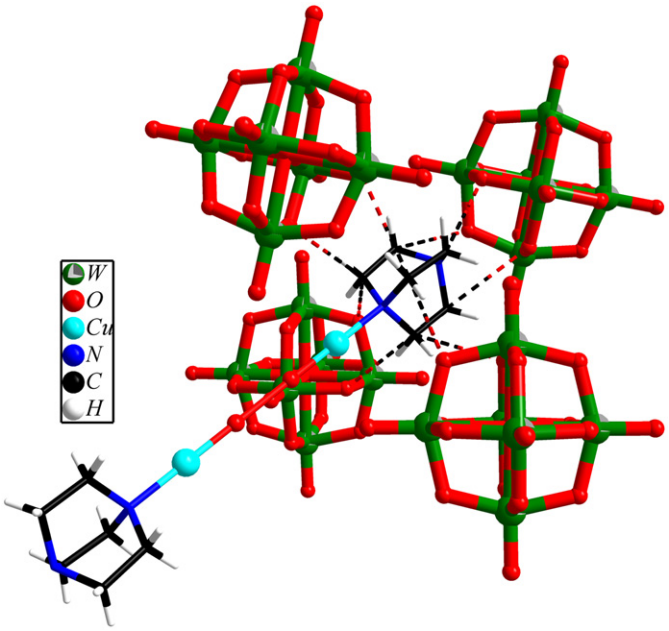

Fig. 2. The representation of the C–H···O hydrogen bonding interactions between the DABCO ligands and the $[W_3^{VI}V_3^{V}O_{19}H]^{4-}$ anions.

Table 2
Hydrogen bonds for complexes **1**, **2** and **3**.

D–H···A	d(D···A)	Symmetry code
Complex **1**		
C1···O3(a)	3.24(4)	a: $(-y,0.5+z,-0.5-x)$
C2···O3(b)	3.23(4)	b: $(1+z,\ 0.5-x,-0.5+y)$
N2···O3(c)		c: $(-y,-1-z,-x)$
Complex **2**		
N2···N3	2.68(4)	
N(1)···O(15)(d)	3.08(3)	d: $(y,x,3-z)$
C(4)···O(8)	3.19(5)	
C(4)···O(13)(e)	3.26(7)	e:$(1-x+y,2-x,z)$
Ow(1)···Ow(3)(f)	2.64(7)	f:$(1-x+y,2-x,z)$
Ow(3)(e)···Ow(2)(g)	3.13(4)	g:$(1-x+y,2-x,z)$
Ow(1)···O(8)	3.00(7)	
Ow(1)···O(12)(h)	2.94(8)	h:$(1-x+y,2-x,z)$
Ow(2)···O(14)	3.05(4)	
Complex **3**		
N(2)···O(14)(i)	2.95(1)	i:$(x,\ y,\ 1+z)$
N(2)···O(12)(i)	2.87(2)	

the carbon atom C(2) (and its symmetry equivalents) interacts with O(3) $(1+z,\ 0.5-x,-0.5+y)$ (and its symmetry equivalents) with bond distance of 3.23(4) Å. Therefore, it means that every carbon atom of the DABCO ligands interacts with the oxygen atoms of the $[W_3^{VI}V_3^{V}O_{19}H]^{4-}$ anions through hydrogen bonds. In addition, the N(2) atom of the DABCO ligand interacts with the O(3) (and its symmetry equivalents) through hydrogen bond with distance of 3.00(3) Å (the hydrogen bonds for **1** are shown in Table 2).

Structure of 2: The X-ray crystallographic study reveals that **2** is composed of $[P_2Mo_{18}^{VI}O_{62}]^{6-}$ clusters, water molecules, organic counterions $[H_2DABCO]^{2+}$ and $[HDABCO]^{+}$. The $[P_2Mo_{18}^{VI}O_{62}]^{6-}$ cluster is a Dawson archetype, consisting of two $\{PMo_9O_{34}\}$ groups joined together by sharing six oxygen atoms (as shown in Fig. 3). There have been extensive studies on the formation of molybdophosphate complexes, various molybdophosphate complexes including $[P_2Mo_5O_{23}]^{6-}$, $[PMo_{11}O_{39}H_3]^{4-}$, $[PMo_9O_{34}H_6]^{3-}$, $[PMo_{12}O_{40}]^{3-}$, $[P_2Mo_{18}O_{62}]^{6-}$ are isolated [5a, 14]. In general, the formation of these heteropoly complexes is said to be pH-dependent. Among the heteropolymolybdate complexes in the Mo–P system, the Keggin- and Dawson-type complexes are of particular interest because of their importance in solution chemistry and their uses as catalysts [5a, 14].

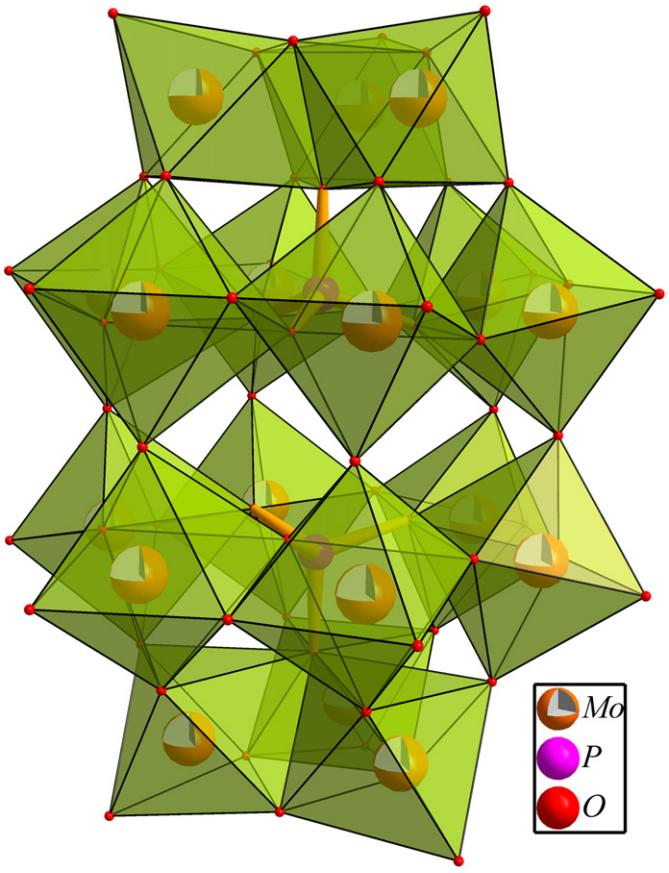

Fig. 3. The polyhedron representation of the $[P_2Mo_{18}^{VI}O_{62}]^{6-}$ anion.

The PO_4 tetrahedron of the $[P_2Mo_{18}^{VI}O_{62}]^{6-}$ cluster has P–O distances of 1.539(13)–1.595(13) Å. Each molybdenum atom has a distorted $\{MoO_6\}$ octahedral coordination environment. The distances of the Mo–O bonds can be divided into three groups: Mo–O_t, 1.708(17)–1.718(15) Å; Mo–O_b, 1.840(15)–1.998(15) Å; Mo–O_c, 2.342(12)–2.360(13) Å. Bond valence sums (BVS) for the molybdenum atoms of **2** were calculated by using parameters given by Brown [12]. Results for the independent molybdenum atoms Mo1, Mo2 and Mo3 are 5.60, 5.90 and 6.10, respectively, which reveals that the oxidation state for the molybdenum atoms is +6. Thus the formula for **2** is $[P_2Mo_{18}^{VI}O_{62}]^{6-}$.

It should be noted that the stacking mode of compound **2** is interesting. As shown in Fig. 4, there exist two different "trimers" in **2**: triangle trimer and linear trimer. The former is constructed from three $[P_2Mo_{18}^{VI}O_{62}]^{6-}$ anions, exhibiting a perfect equilateral triangle motif, while the latter is constructed from two $[HDABCO]^{+}$ and one $[H_2DABCO]^{2+}$ counterions packed linearly along the *c*-axis in a $[HDABCO]^{+}\cdots[HDABCO]^{+}\cdots[H_2DABCO]^{2+}$ linking fashion. The centroid–centroid distances of any two of the three anions of the triangle trimer is characterized by separation of 13.2621(3) Å, while the centroid–centroid distances of the two neighboring DABCO counterions of the linear trimer is 5.13(4) Å. It should be noted that the two neighboring DABCO counterions of the linear trimer interact with each other through strong N–H···N hydrogen bonding interactions with N···N distance of

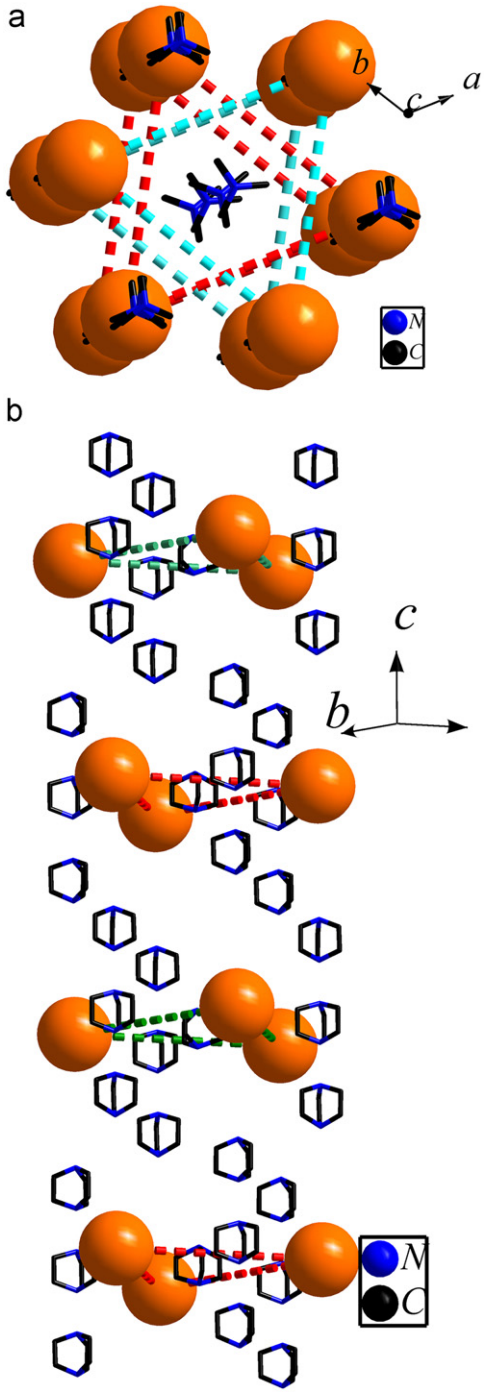

Fig. 4. (a) The upper view of the topological representation of the packing motif in compound **2**. (b) The side view of the packing motif in compound **2**. The big ball represents the $[P_2Mo^{VI}_{18}O_{62}]^{6-}$ anions.

2.68(4) Å, thus there is only one hydrogen atom in the middle of each two neighboring DABCO counterions. As shown in Fig. 4, each $[P_2Mo^{VI}_{18}O_{62}]^{6-}$ anion of the triangle trimer is surrounded by three linear trimers, while each linear trimer is surrounded by three $[P_2Mo^{VI}_{18}O_{62}]^{6-}$ anion of the triangle trimers. The triangle trimers act as building blocks stacked along the *c*-axis. However, the upper triangle trimer could not fully overlap the lower one, for the lower one was rotated about $\pm 60^{\circ}$. Therefore, the triangle trimers are stacked along the *c*-axis into an –A–B–A–B– stacking mode. Detailed analysis also revealed that the linear trimer and the $[P_2Mo^{VI}_{18}O_{62}]^{6-}$ anions of the triangle trimers are arranged alternately along the *c*-axis into a chain structure through N–H···O hydrogen bonding interactions with N(1)…O(15) $(y,x,3-z)$ (and its symmetry equivalents) distance of 3.08(3) Å.

Except the linear trimer, there still exist discrete organic counterions $[H_2DABCO]^{2+}$. The discrete $[H_2DABCO]^{2+}$, which is just located at the inversion center of the triangle trimer of $[P_2Mo^{VI}_{18}O_{62}]^{6-}$ anions, exhibits C–H···O hydrogen bonding interactions with the three $[P_2Mo^{VI}_{18}O_{62}]^{6-}$ anions with C(4)···O(8), C(4)···O(13)$(1-x+y,2-x,z)$ (and their symmetry equivalents) distances of 3.19(5) and 3.26(7) Å, respectively.

There is a dinuclear water cluster $(H_2O)_2$ in compound **2**, which is constructed from Ow(1) and Ow(3) water molecules. The Ow(1) interacts with the Ow(3)$(1-x+y,2-x,z)$ with hydrogen bond distance of 2.64(7) Å, thus, a dinuclear water cluster is formed. Crystallographic analysis reveals that there exist complex hydrogen bonding interactions between oxygen atoms of the water cluster $(H_2O)_2$ and oxygen atoms of the $[P_2Mo^{VI}_{18}O_{62}]^{6-}$ anions. Ow(1) (and its symmetry equivalents) interacts with the O(8) and O12$(1-x+y,2-x,z)$ (and their symmetry equivalents) with bond distances of 3.00(7) and 2.94(8) Å, respectively. In addition, Ow(3)$(1-x+y,2-x,z)$ of the water cluster $(H_2O)_2$ interacts with the dissociated water molecule Ow(2) $(1-x+y,2-x,z)$ through hydrogen bonding interactions with bond distance of 3.13(4) Å. There also exists hydrogen bonding interactions between Ow(2) (and its symmetry equivalents) and O(14) (and its symmetry equivalents) with bond distances of 3.05(4) Å (the hydrogen bonds for **2** are shown in Table 2).

Structure of 3: The X-ray crystallographic study reveals that **3** consists of an infinite inorganic $[Mo_{7.5}W_{0.5}O_{27}]_{\infty}$ chain, transition metal coordination fragments $[Cu(DABCO)]^{+}$ and protonated water molecules. The chain is composed of the $[Mo_{7.5}W_{0.5}O_{27}]^{5-}$ clusters, each of which exhibits the framework structure of the $[Mo_8O_{27}]^{5-}$ [9b] with one position of the molybdenum atom occupied by disordered Mo and W with equivalent occupancy factor of 0.5. The $[Mo_{7.5}W_{0.5}O_{27}]^{5-}$ cluster is constructed from eight distorted $\{MO_6\}$ octahedra joined together by sharing edges. The existence of the mixed metal isopolyanions (molybdotungstates) have been suggested by the aqueous or nonaqueous solution studies including $[Mo_6W_6O_{41}]^{10-}$, $[Mo_3W_{15}O_{60}H_3]^{9-}$, $[(H_2)MoW_{11}O_{40}]^{6-}$, $[Mo_3W_3O_{19}]^{2-}$, $[H_2Mo_2W_{10}O_{30}]^{5-}$, $[MoW_5O_{19}]^{2-}$, etc. [5a].

The M–O bond distances of the $[Mo_{7.5}W_{0.5}O_{27}]^{5-}$ cluster can be divided into three groups: M–O_t 1.702(9)–1.722(9) Å, M–O_b 1.743(8)–2.216(7) Å, M–O_c, 2.270(7)–2.437(7) Å. Bond valence sums (BVS) for the molybdenum atoms and the tungsten atoms of **3** were calculated by using parameters given by Brown [12]. Results for the independent molybdenum atoms Mo1, Mo2, Mo3 and Mo4 are 5.92, 5.90, 5.86 and 5.91, while result for the independent tungsten atom W1 is 5.92, which reveals that the oxidation state of the molybdenum and tungsten atoms of the $[Mo_{7.5}W_{0.5}O_{27}]^{6-}$ is +6. Thus the formula for **3** is $[Mo^{VI}_{7.5}W^{VI}_{0.5}O_{27}]^{6-}$.

A feature of **3** is that the $[Mo_{7.5}W_{0.5}O_{27}]^{6-}$ clusters are connected by sharing corners into an inorganic chain which is then decorated by $[Cu(HDABCO)]^{2+}$ TMCs, as shown in Fig. 5. Between every two $[Mo_{7.5}W_{0.5}O_{27}]^{6-}$ clusters in the chain, there not only exists an oxygen atom O(5) as bridge, but also exist two $[Cu(HDABCO)]^{2+}$ TMCs as bridges. Alternatively, there are two different types of bridges in the chain: oxygen bridges and TMC bridges. The TMC of **3** exhibits a tetrahedral coordination environment, it receives contributions from one nitrogen donor of DABCO ligand (Cu–N bond distance: 1.986(9) Å) and three oxygen donors from two anions (Cu–O bond distances: 1.868(8)–2.756(9) Å). Thus TMCs in **3** act as bridges interconnecting the neighboring POMs into a straight chain structure along the *a*-axis (Fig. 5). Bond valence sums (BVS) for copper atoms of **3** were calculated [13]. Result for the independent copper atom Cu1 is

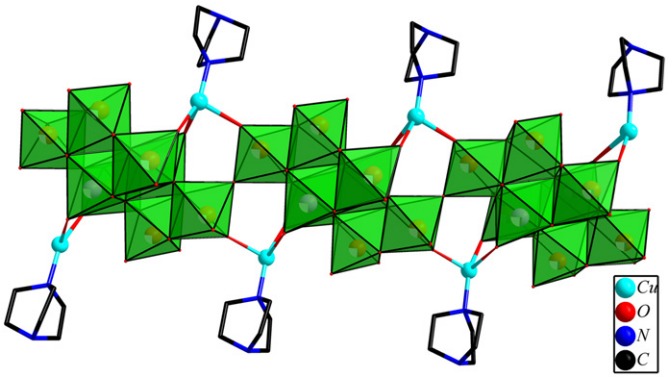

Fig. 5. The representation of the 1-D $[Mo_{7.5}W_{0.5}O_{27}]_{\infty}$ chain structure decorated by $[Cu(DABCO)]^{+}$ TMCs in compound **3**.

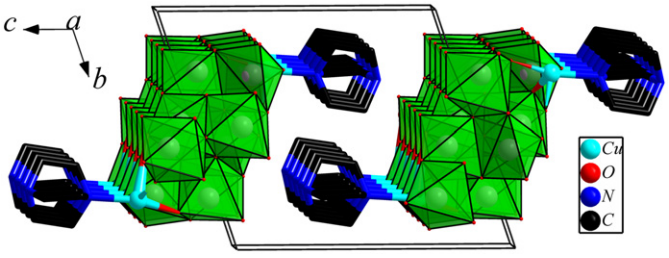

Fig. 6. The representation of the 2-D supramolecular layer structure in compound **3**.

1.06, which reveals that the oxidation state of the copper atoms of **3** is +1.

The most unusual feature of **3** is the stacking mode of the infinite chain, as shown in Fig. 6. The infinite chain decorated by $[Cu(HDABCO)]^{2+}$ TMCs exhibits a chair form, adjacent chains with DABCO ligands are packed in an orderly manner along the *c*-axis into a supramolecular layer structure.

Crystallographic analysis reveals that the packing of **3** comes from the hydrogen bonding interactions between the nitrogen atoms of DABCO ligands and the oxygen atoms of $[Mo_{7.5}W_{0.5}O_{27}]^{6-}$ anions. N(2) (and its symmetry equivalents) performing as the hydrogen donor interacts with the O(14) (*x*, *y*, 1+*z*) and O(12) (*x*, *y*, 1+*z*) (and their symmetry equivalents) as hydrogen acceptor with bond distances of 2.95(1) and 2.87(2) Å, respectively (the hydrogen bonds for **3** are shown in Table 2). These strong hydrogen bonds link the infinite chain into a supramolecular layer structure.

It should be noted that there was an isopolyanion compound reported by Zhang et al. that is isostructural with compound **3** [9b]. The biggest difference between these two compounds is the building blocks of the two compounds, one is isopolyanion $[Mo_8O_{27}]^{5-}$, the other is mixed metal isopolyanion $[Mo_{7.5}W_{0.5}O_{27}]^{5-}$.

3.2. Characterizations of compounds

3.2.1. XRD analysis

The XRD analyses have already been done to confirm the phase purity for **1**, **2** and **3** (Fig. s1–s3). The experimental patterns for compounds **1**, **2** and **3** are in good agreement with the simulated patterns, respectively, indicating that the phase purity for **1**, **2** and **3** are good.

3.2.2. XPS analysis

The XPS spectra for **1** present two overlapped peaks at 35.5 V and 37.6 eV in the W4f region which should be ascribed to W^{6+} (Fig. s4) [15]. The XPS spectra for **1** also present two peaks at 517.0, 524.7 eV in the V2*p* region, which should be ascribed to the V^{5+} (Fig. s4) [15].

The XPS spectrum for **2** presents two peaks in the Mo 3*d* region at 236.1 and 232.8 eV, which should be ascribed to Mo^{6+} (Fig. s5) [15]. The XPS spectra of **3** present two peaks 236.2 and 233.0 eV, which should be ascribed to Mo^{6+} (Fig. s6) [15]. The XPS spectra of **3** presents two peaks 37.6 and 35.5 eV, which should be ascribed to W^{6+} (Fig. s6) [15].

3.2.3. TG analysis

The TG curve for compound **1** was recorded from room temperature to 800 °C. The curve is very hard to be divided into different stages (Fig. s7). It continuously decreases until 529 °C with weight loss about 19.0%, corresponding to the loss of water molecules and DABCO ligands in **1** (calc.: 17.8%).

The TG curve for compound **2** was recorded from room temperature to 800 °C. The curve is very hard to be divided into different stages (Fig. s8). It continuously decreases until 604 °C with weight loss about 17.6%, corresponding to the loss of water molecules and DABCO ligands in **2** (calc.: 19.4%).

4. Conclusion

The synthesis and characterization of $[W_3^{VI}V_3^{V}O_{19}H]\{[Cu(HDABCO)]_2(H_2O)\}$ (**1**), $[P_2Mo_{18}^{VI}O_{62}][DABCO][H_2DABCO]_3\cdot 12\,H_2O$ (**2**) and $[Mo_{7.5}^{VI}W_{0.5}^{VI}O_{27}][Cu(HDABCO)]_2\cdot 2\,H_3O\cdot 2\,H_2O$ (**3**) reinforce the observation that the same organonitrogen combining with the different POMs will yield different supramolecular networks. It is evident that the incorporation of organic components and POMs combined with hydrothermal technique affords a powerful method for the supramolecular networks.

Acknowledgments

This work was supported by National Natural Science Foundation of China under Grant no. 21003056. We also thank the grant from Jilin University, no. 200903123.

Appendix A. Supplementary material

Supplementary data associated with this article can be found in the online version at doi:10.1016/j.jssc.2010.09.038.

References

[1] (a) J.M. Lehn, in: Supramolecular Chemistry, VCH, New York, 1995;
(b) F. Vögtle, in: Supramolecular Chemistry, Wiley, Chichester, 1991;
(c) J.-M. Lehn, in: Comprehensive Supramolecular Chemistry, Pergamon, New York, 1996.
[2] (a) J.M. Lehn, Angew. Chem. Int. Ed. Engl. 29 (1990) 1304;
(b) J.M. Lehn, in: Supramolecular Chemistry, VCH, Weinheim, 1995.
[3] (a) C.N.R. Rao, S. Natarajan, R. Vaidhyanathan, Angew. Chem. Int. Ed. 43 (2004) 1466;
(b) O.M. Yaghi, M. O'Keeffe, N.W. Ockwig, H.K. Chae, M. Eddaoudi, J. Kim, Nature 423 (2003) 705;
(c) B.F. Abrahams, A. Hawley, M.G. Haywood, T.A. Hudson, R. Robson, D.A. Slizys, J. Am. Chem. Soc. 126 (2004) 2894;
(d) J.L.C. Rowsell, O.M. Yaghi, Microporous Mesoporous Mater. 73 (2004) 3.
[4] S.V. Kolotuchin, E.E. Fenlon, S.R. Wilson, C.J. Loweth, S.C. Zimmerman, Angew. Chem. Int. Ed. 34 (1995) 2654.
[5] (a) M.T. Pope, in: Heteropoly Isopoly Oxometalates, Springer-Verlag, Berlin, 1983;
(b) M.T. Pope, A. Müller, Angew. Chem. Int. Ed. Engl. 30 (1991) 34;
(c) Chem. Rev. 98 (1998) 1;
(d) M.T. Pope, A. Müller, in: Polyoxometalates: From Platonic Solids to Anti-Retro Viral Activity, Kluwer, Dordrecht, The Netherlands, 1994;

(e) M.T. Pope, A. Müller, in: Polyoxometalate Chemistry: From Topology via Self-Assembly to Applications, Kluwer, Dordrecht, The Netherlands, 2001;
(f) T. Yamase, M.T. Pope, in: Polyoxometalate Chemistry for Nano-Composite Design, Kluwer, Dordrecht, The Netherlands, 2002;
(g) P.J. Hagrman, D. Hagrman, J. Zubieta, Angew. Chem. Int. Ed. Engl. 38 (1999) 2638.
[6] (a) P.Q. Zheng, Y.P. Ren, L.S. Long, R.B. Huang, L.S. Zheng, Inorg. Chem. 44 (2005) 1190;
(b) X.L. Wang, C. Qin, E.B. Wang, Y.G. Li, N. Hao, C.W. Hu, L. Xu, Inorg. Chem. 43 (2004) 1850;
(c) C.P. Pradeep, D.L. Long, G.N. Newton, Y.F. Song, L. Cronin, Angew. Chem. Int. Ed. 47 (2008) 4388;
(d) Z.H. Yi, X.B. Cui, X. Zhang, G.D. Yang, J.Q. Xu, X.Y. Yu, H.-H. Yu, W.J. Duan, J. Mol. Struct. 891 (2008) 123;
(e) T.R. Veltman, A.K. Stover, A.N. Sarjeant, K.M. Ok, P.S. Halasyamani, A.J. Norquist, Inorg. Chem. 45 (2006) 5529;
(f) R. Atencio, A. Briéno, X. Galindo, Chem. Commun. (2005) 637;
(g) R. Atencio, A. Bricéno, P. Silva, J.A. Rodríguez, J.C. Hanson, New J. Chem. 31 (2007) 33.
[7] (a) H.K. Chae, D.Y. Siberio, J. Kim, Y. Go, M. Eddaoudi, A.J. Matzger, M. O'Keeffe, O.M. Yaghi, Nature 427 (2004) 523;
(b) Z. Han, Y. Zhao, J. Peng, A. Tian, Q. Liu, J. Ma, E. Wang, N. Hu, CrystEngComm 7 (2005) 380;
(c) J.S. Seo, D. Whang, H. Lee, S.I. Jun, J. Oh, Y.J. Jeon, K. Kim, Nature 404 (2000) 982;
(d) O. Kahn, C. Martinez, Science 279 (1998) 44;
(e) C. Janiak, Angew. Chem. Int. Ed. Engl. 36 (1997) 1431.
[8] (a) C. Streb, D.L. Long, L. Cronin, CrystEngComm 8 (2006) 629;
(b) V. Coué, R. Dessapt, M. Bujoli-Doeuff, M. Evain, S. Jobic, Inorg. Chem. 46 (2007) 2824;
(c) T. Akutagawa, D. Endo, S.I. Noro, L. Cronin, T. Nakamura, Coord. Chem. Rev. 251 (2007) 2547;
(d) X.Y. Zhao, D.D. Liang, S.X. Liu, C.Y. Sun, R.G. Cao, C.Y. Gao, Y.H. Ren, Z.M. Su, Inorg. Chem. 47 (2008) 7133;
(e) Y. Wang, J.H. Yu, M. Guo, R.R. Xu, Angew. Chem. Int. Ed. 42 (2003) 4089.
[9] (a) R. Dessapt, M. Collet, V. Coué, M. Bujoli-Doeuff, S. Jobic, C. Lee, M.H. Whangbo, Inorg. Chem. 48 (2009) 574;
(b) R.Q. Fang, Y.F. Zhao, X.M. Zhang, Inorg. Chim. Acta 359 (2006) 2023.
[10] H.K. Chae, W.G. Klemperer, V.W. Day, Inorg. Chem. 28 (1989) 1424.
[11] (a) Y.N. Zhang, B.B. Zhou, Y.G. Li, Z.H. Su, Z.H. Zhao, Dalton Trans. (2009) 9446;
(b) S. Reinoso, L.F. Piedra-Garza, M.H. Dickman, A. Praetorius, M. Biesemans, R. Willem, U. Kortz, Dalton Trans. 39 (2010) 248;
(c) C.R. Graham, L.S. Ott, R.G. Finke, Langmuir 25 (2009) 1327.
[12] I.D. Brown, in: M. O'Keefe, A. Navrotsky (Eds.), Structure and Bonding in Crystals, vol. 2, Academic Press, New York1981, pp. 1–30.
[13] N.E. Brese, M. O'Keefe, Acta Crystallogr. B47 (1991) 192.
[14] S. Hemino, M. Hashimoto, T. Ueda, Inorg. Chim. Acta 284 (1999) 237.
[15] C.D. Wagner, W.M. Riggs, L.E. Davis, J.F. Moulder, G.E. Muilenberg, in: Handbook of X-ray Photoelectron Spectroscopy, Perkin-Elmer Corp, MI, 1978.